

1 Supplementary Figure Legends

2 Supplementary Figure 1: Differentiation markers

3 a) Representative images during differentiation of SGBS adipocytes along with expression
4 for several marker genes during the four time points ($n = 3$ replicates, data shown are mean
5 expression estimates \pm SD). b) Representative images during differentiation of iPSC derived
6 hypothalamic neurons along with expression of several marker genes during the three time
7 points ($n = 3$ replicates, data shown are mean expression estimates \pm SD).

8

9 Supplementary Figure 2: Features of functional annotations

10 a) Six fuzzy-c means clusters were identified for adipose and b) hypothalamic DEGs from
11 the RNA-seq time course. The number of genes comprising each cluster, along with scaled
12 expression across the time points is shown. c) Overview of median interaction length and
13 number of interactions per time-point in the replicate-merged cHi-C datasets. Number of
14 ATAC-seq peaks from the replicate-merged time points. d) Bar plot depicting proportion of
15 promoter-promoter interactions in merged cHi-C libraries. e,f) The promoter-distal ends of
16 interactions are enriched for functional ChIP-seq peaks and ATAC-seq peaks compared to a
17 distribution of randomly chosen, number-matched set of non-promoter Mbol fragments
18 within mappable genomic regions ($n = 100$ iterations). The fold change of the observed
19 overlap over 100 randomized sets is presented. ChIP-seq datasets were obtained from
20 Adipose Nuclei (E063) and Fetal Brain (E081) repositories from the Roadmap Epigenomics
21 project. (* $p < 0.05$; two-sided Z-test) Data shown as the average of the 100 randomizations \pm
22 SD g) Genes were binned based on upregulation or downregulation across each time point.
23 Plotted are the changes in interaction score or normalized ATAC-seq reads for ATAC peaks
24 connected through these genes via a significant cHi-C peak between each time point.
25 boxplot center line, median; box limits, upper and lower quartiles; whiskers, 1.5x
26 interquartile range; outliers not shown * $p < 0.05$; two-sided Mann-Whitney U test. Adipose
27 values for each bin (Day 0-2) $n = 2,205$ up, $n = 3,998$ down, $n = 26,752$ not DE; (Day 2-8) $n =$
28 653 up, $n = 717$ down, $n = 31,575$ not DE, (Day 8-16) $n = 545$ up, $n = 849$ down, $n = 31,551$
29 not DE; Neuron values for each bin (Day 12-16) $n = 1,588$ up, $n = 2,457$ down, $n = 20,726$
30 not DE; (Day 16-27) $n = 1,495$ up, $n = 363$ down, $n = 22,913$ not DE.

31

32 Supplementary Figure 3: Characterizing Adipocyte Differentiation using Genomic
33 Annotations

34 a) Time points for data collection b) Adipose DEGs were grouped via fuzzy-c means
35 clustering and the top three clusters with highest membership scores are illustrated. The
36 number of genes in each cluster and scaled expression across the four differentiation time
37 points is depicted. c) Significant KEGG pathway terms identified using Enrichr for the top
38 three clusters (Fisher's Exact Test; p values are adjusted for multiple tests). d) Heatmap of
39 gene expression depicting genes from each of the top three clusters that are members of the
40 enriched KEGG pathway terms. The leftmost colored bar indicates cluster membership and
41 each column is an RNA-seq replicate. e-g) HSV transformation of expressed genes, ATAC-seq
42 peaks, and cHi-C interactions across differentiation. The three nodes of each pattern
43 represent day 0, day 2, and day 16 of adipose differentiation. The distance of each point
44 from the center of the circle represents maximum \log_2 fold change, and color transparency
45 represents the relative number of reads for that data point. Below, heatmaps of Pearson's r

46 correlation coefficients estimate overall similarity between time points. h) On average, a
47 promoter interacts with 3-4 ATAC-seq peaks via a cHi-C interaction across time
48 (interactions and ATAC peaks were not required to be significant at the same time point). i)
49 View of cHi-C interactions from the promoter of the *IRS2* gene, which becomes upregulated
50 between differentiation days 0-2. ATAC-seq reads and peaks from day 0 and day 2 are also
51 shown.

52

53 Supplementary Figure 4: MPRA enhancer activity is supported

54 a) MPRA enhancers are enriched for Epigenome Roadmap's 15 state ChromHMM functional
55 marks in adipose nuclei or fetal brain compared to all tested variants b) MPRA enhancers
56 are enriched for presence in cHi-C interactions, number of interactions per enhancer, and
57 open chromatin compared to non-significant regions. (* $p < 0.05$; two-sided Student's t -test)
58 c) Luciferase assay results for ~1 kb sized regions containing an EMVar. Regions were
59 chosen at random, and represent a full spectrum of MPRA enhancer p values. Because of
60 this, non-EMVar rs1026737 and rs10000940 were included because they had very low and
61 high enhancer p values, respectively. If the allele that was captured was not a significant
62 enhancer, the result is colored with a grey background. Interestingly, for the rs4430895
63 region, we were able to clone both alleles, and although neither allele was an enhancer
64 using the luciferase assay, the allele predicted to be stronger with MPRA had higher Luc2
65 expression compared to the weak allele. $n = 9$ independent replicates for all constructs
66 except $n = 12$ independent replicates for rs2836753_G, rs1800437_G, rs6091542_T +
67 rs6096971_A + rs6096972_G, rs3800231_T, rs41303827_G, rs843812_A, rs7146955_A,
68 rs7030846_T, rs1406256_C, rs78575557_A and rs794364_A tested in in 3T3-L1 cells.
69 boxplot center line, median; box limits, upper and lower quartiles; whiskers, 1.5x
70 interquartile range. rs794364_A_3T3 $p = 4.8e-3$; rs794364_A_HT22 $p = 4.7e-3$;
71 rs7146955_A_HT22 $p = 1.1e-3$; rs56358680_A_HT22 $p = 2.3e-4$; rs56358680_A_3T3 $p =$
72 $1.7e-3$; rs4788211_A_HT22 $p = 8.5e-5$; rs4788211_A_3T3 $p = 3.8e-6$; rs2382538_A_3T3 $p =$
73 $7.0e-4$; rs2382538_A_HT22 $p = 1.96e-8$; rs1800437_G_3T3 $p = .02$; rs1800437_G_HT22 $p =$
74 $7.72e-6$; rs13204087_C + rs13220728_T_3T3 $p = 1.8e-4$; rs13204087_C +
75 rs13220728_T_HT22 $p = 8.4e-5$; rs116735807_T_3T3 $p = 3.3e-3$; rs116735807_T_HT22 $p =$
76 $2.3e-10$; rs1026737_T_HT22 $p = 2.0e-4$; rs1026737_T_3T3 $p = 2.6e-7$; rs3800231_T_3T3 $p =$
77 $7.0e-3$

78

79 Supplementary Figure 5: Transcription factors in obesity associated loci and additional
80 analysis of chromosome 16

81 a) (left) Position weight matrices and identifiers for enriched transcription factor motifs
82 from HOMER. Each motif was enriched in either MPRA adipose or brain enhancers (HOMER
83 adjusted p value < 0.05 ; Binomial Test). (right) Transcription factors are connected to a BMI
84 relevant phenotype with a line if these factors play a role in that biological process
85 (significant in both brain and adipose = grey circle, significant in adipose = yellow, and
86 significant in brain = blue). b) s-LDSC estimated proportion of total heritability explained
87 per chromosome is depicted along with heritability enrichment values. data shown are
88 percent heritability explained \pm SEM (LD score regression with a block jackknife approach)
89 c) Number of EMVars compared to the number of variants tested with MPRA stratified per
90 chromosome.

91

92 Supplementary Figure 6: Haplotype information and SNP specific interactions for *ATP2A1*
93 locus EMVars

94 a)(left) Summary information for all 10 EMVars identified in both the *SBK1* and *ATP2A1* loci.
95 Two SNPs in the *SBK1* region were neither eQTLs nor did they participate in cHi-C
96 interactions and were thus removed from future consideration. (right) Allele frequencies
97 and haplotype information in the CEU population for all EMVars in the *ATP2A1* locus
98 (LDhap tool: <https://ldlink.nci.nih.gov>). The lead risk variant, rs3888190-A, is outlined in
99 blue. b) MPRA allele specific activity levels for EMVars within the *ATP2A1* locus and *SBK1*
100 locus in adipose or brain libraries. Data presented are the average activity for each barcode
101 across independent experiments. *reached $q < 0.05$ in at least half of all independent
102 experiments or in both biological replicates. exact p values per replicate are presented in
103 the Supplementary Tables; two-sided Mann-Whitney U test. c) Promoter interactions
104 stemming from each EMVar in the *ATP2A1* locus at any time point in both brain and adipose
105 cells. Location of variant is indicated by a red line (b,c) Adipose cHi-C data=yellow, Neuronal
106 cHi-C data = blue

107

108 Supplementary Figure 7: A high level of sharing exists between independent enhancer
109 deletions

110 a) Venn Diagrams depicting numbers of significantly differentially expressed genes between
111 enhancer deletions and WT cells at each time point. The Jaccard Index is a representation of
112 sharing on a scale of 0-1, where 1 is complete sharing and 0 is no sharing. b) Heatmap
113 showing the Pearson r correlations between \log_2 FC of all expressed autosomal genes in the
114 genome for the two enhancer deletion lines compared to WT cells. c) Gene Ontology
115 enrichments for differentially expressed genes that were significantly upregulated or
116 downregulated at two time points during the differentiation. Corresponding volcano plots
117 show directionality and numbers of the differentially expressed genes. (Fishers Exact Test;
118 FDR adjusted p values are presented) d) Locations of CRISPRi guides for each condition.
119 Guides were designed to target the 3'UTR of *SBK1*, the promoter of *GAPDH* as a positive
120 control, and a region downstream of *TUFM* as a negative control. Cells were transfected and
121 isolated via FACS based on the presence of either the Cas9 expressing BFP plasmid (BV421-
122 A) and/or the GFP expressing guide plasmid (FITC-A). The lower left FACS panel represents
123 cells that were not expressing BFP or GFP as a gating control. The lower middle FACS panel
124 represents BFP positive cells and the lower right panel represents double positive BFP/GFP
125 expressing cells.

126

127

128

129

130

131

132

Supplementary Figure 1

a

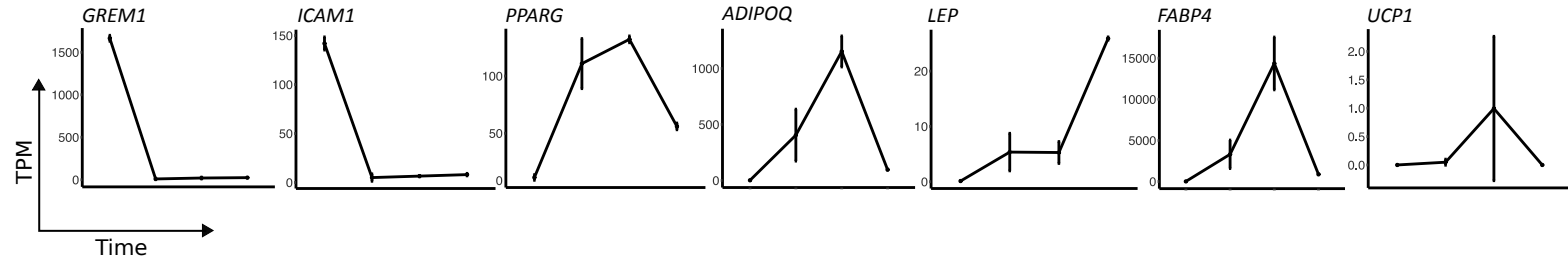
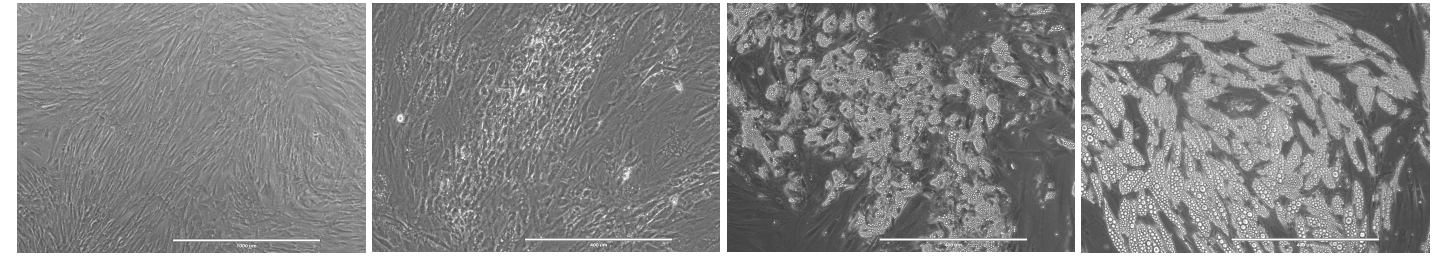
Adipose

D0 (1000um)

D2 (400um)

D8 (400um)

D16 (400um)



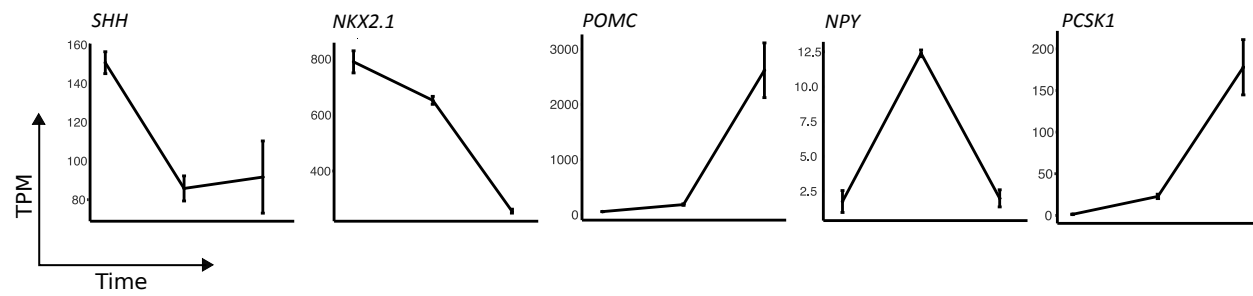
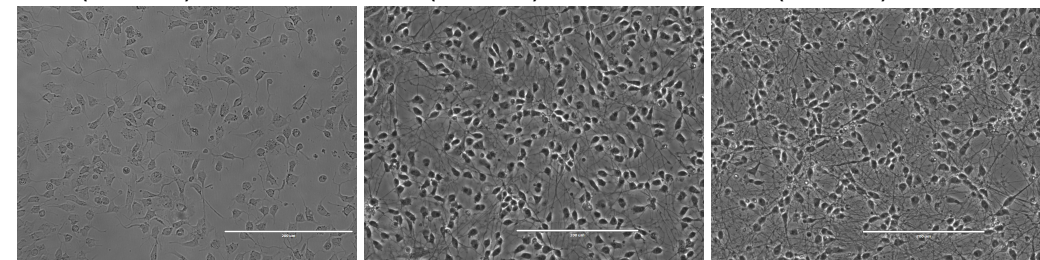
b

Hypothalamic Neurons

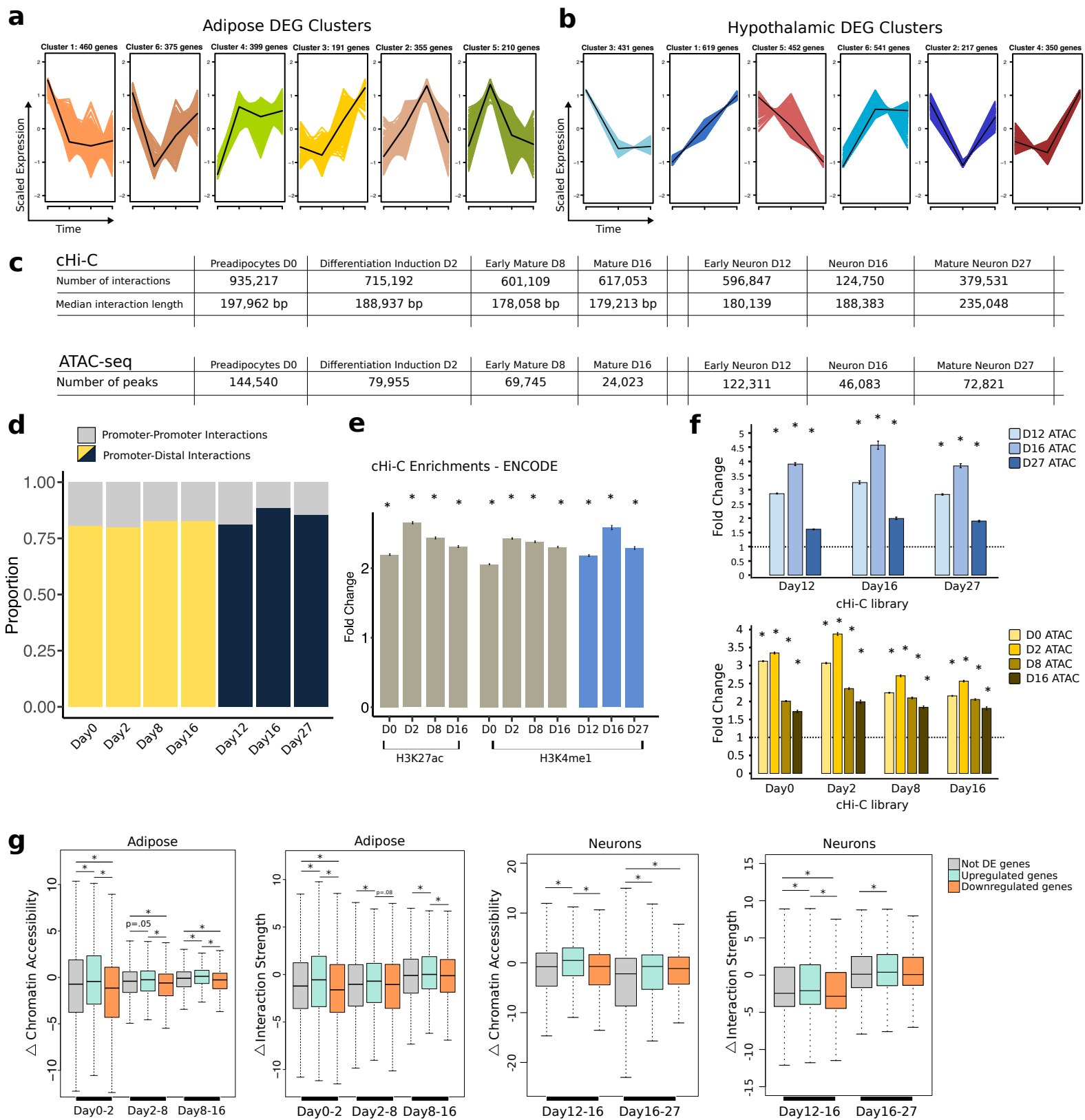
D12 (200um)

D16 (200um)

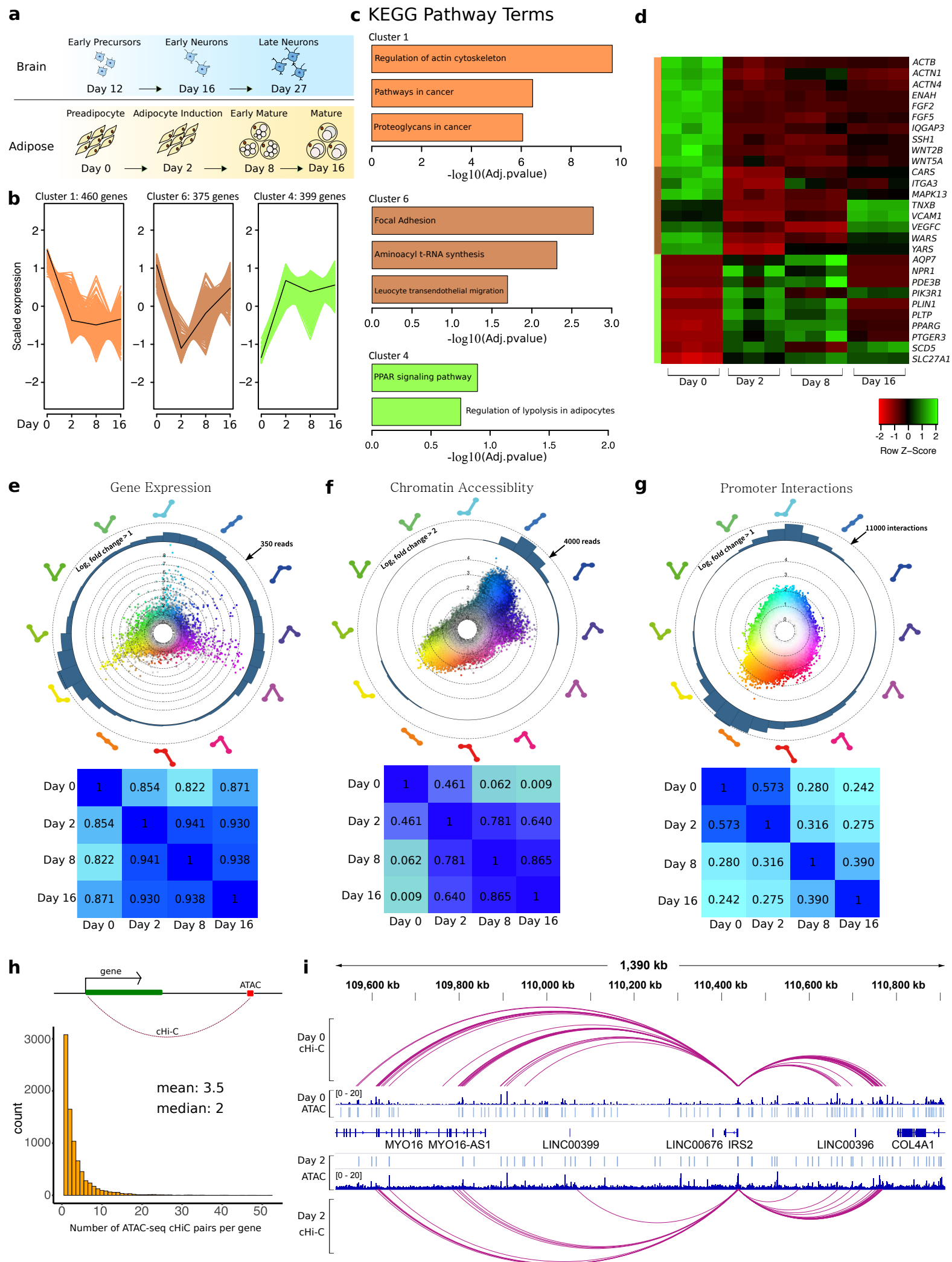
D27 (200um)



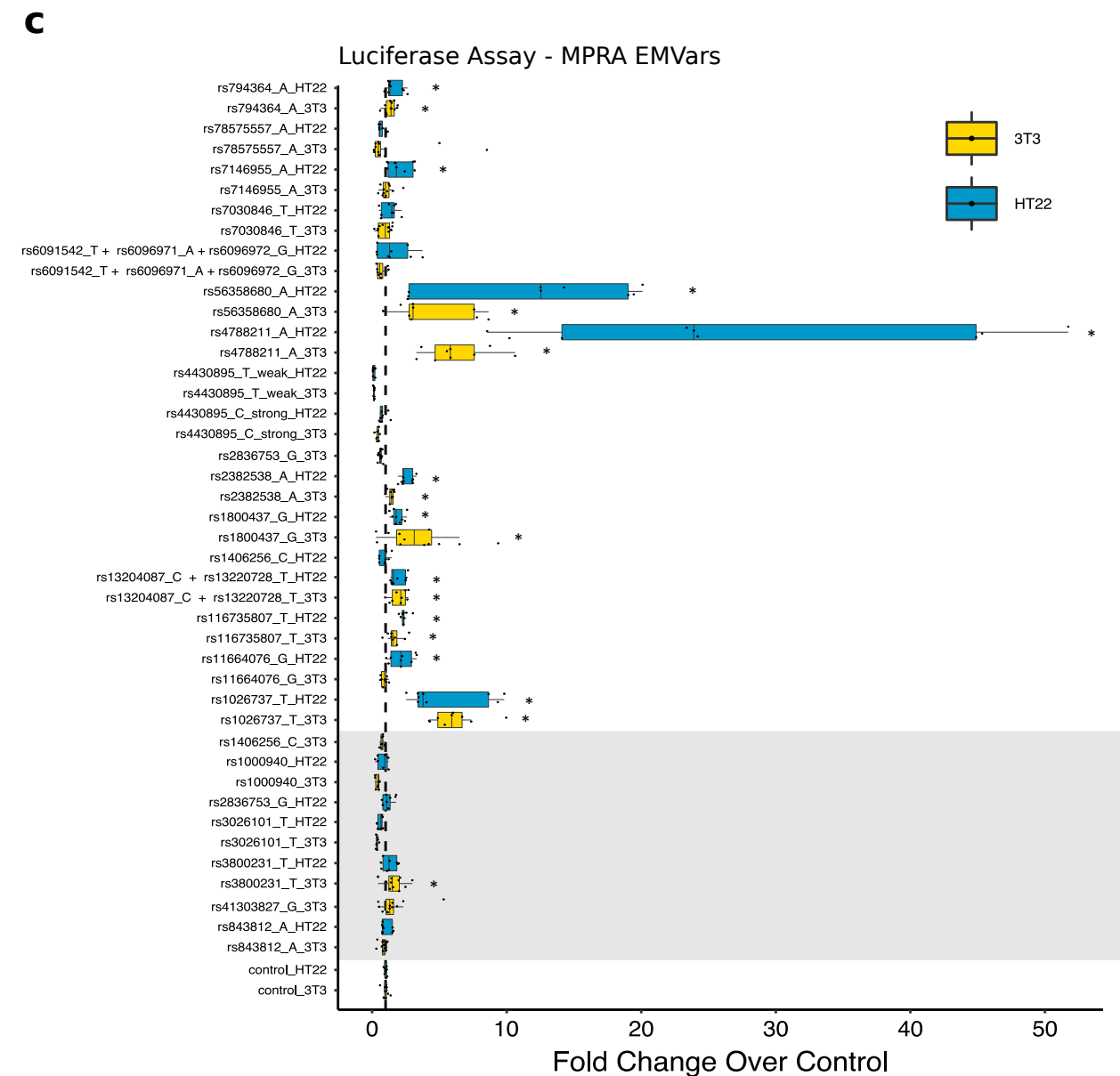
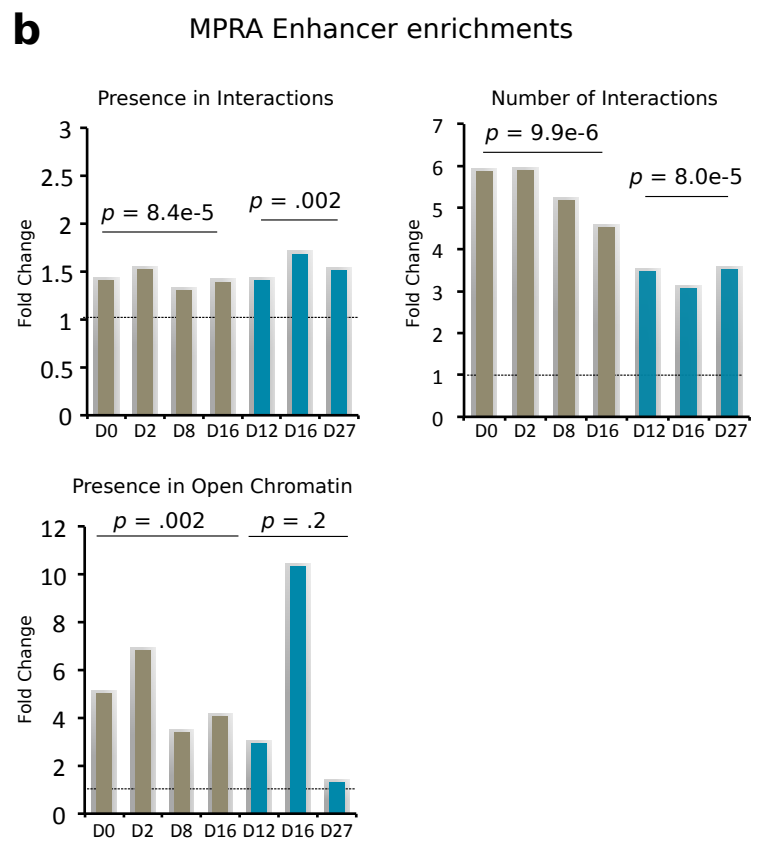
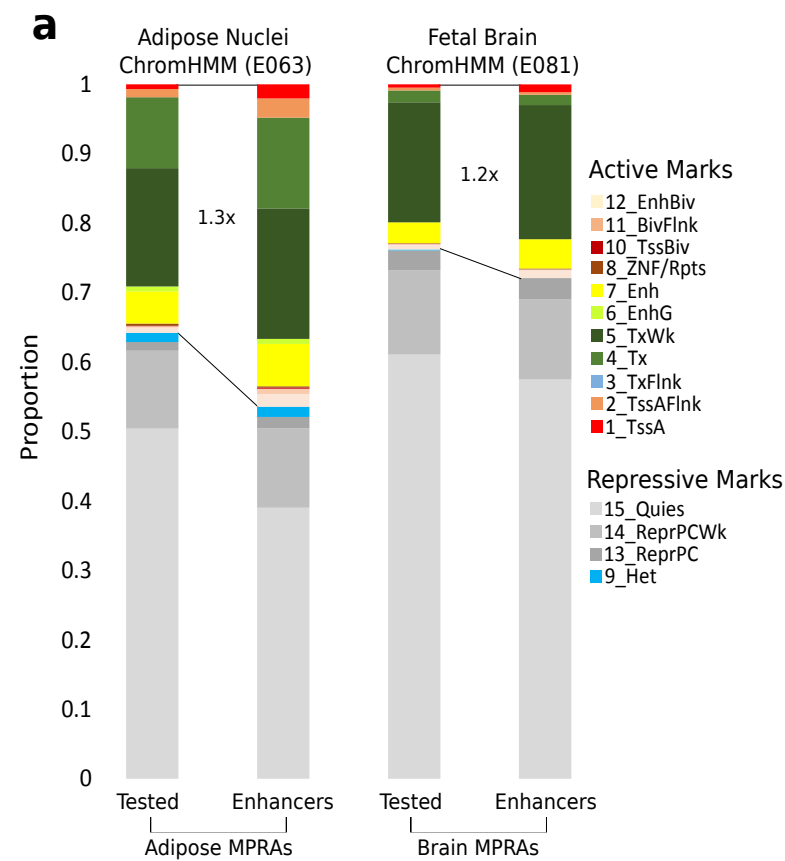
Supplementary Figure 2



Supplementary Figure 3

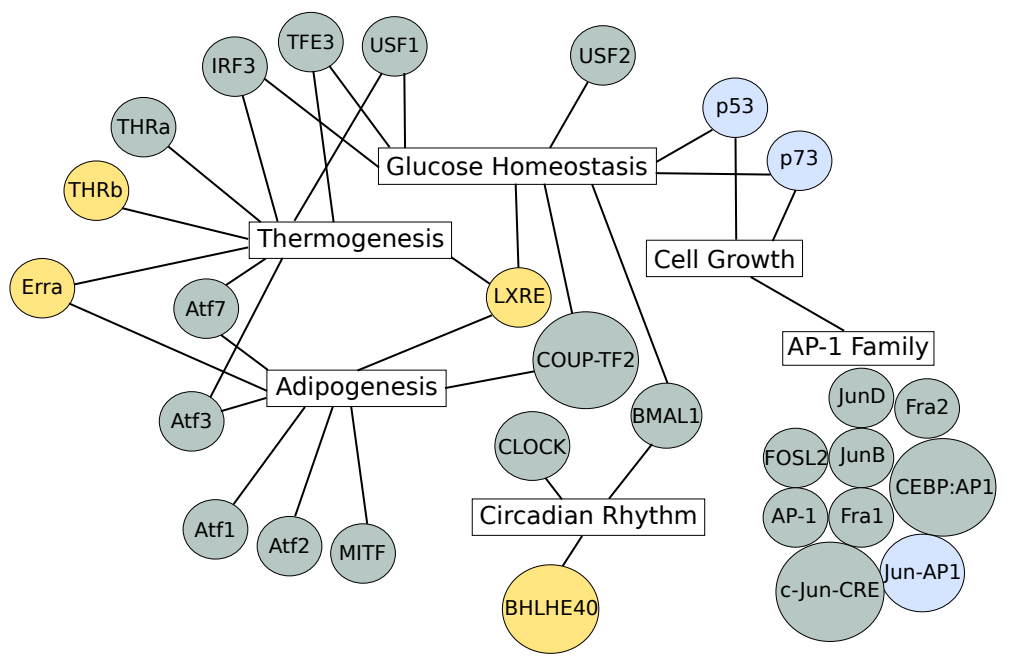
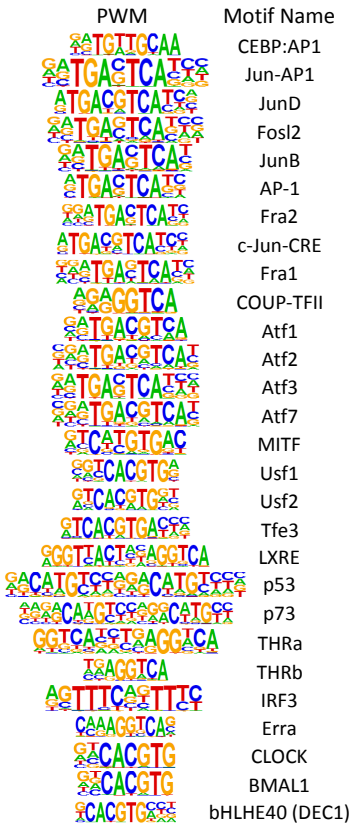


Supplementary Figure 4

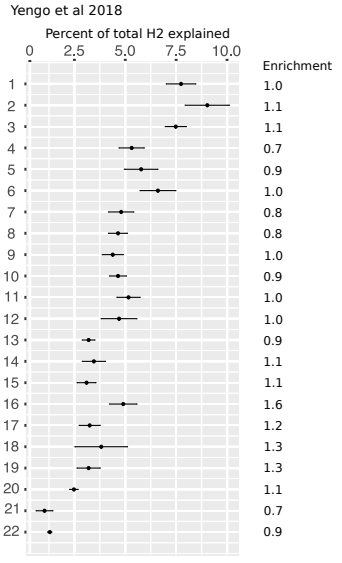
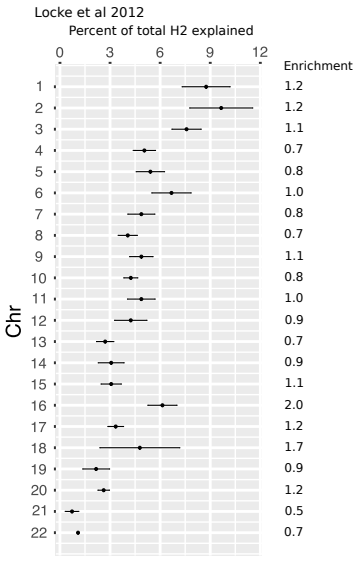


Supplementary Figure 5

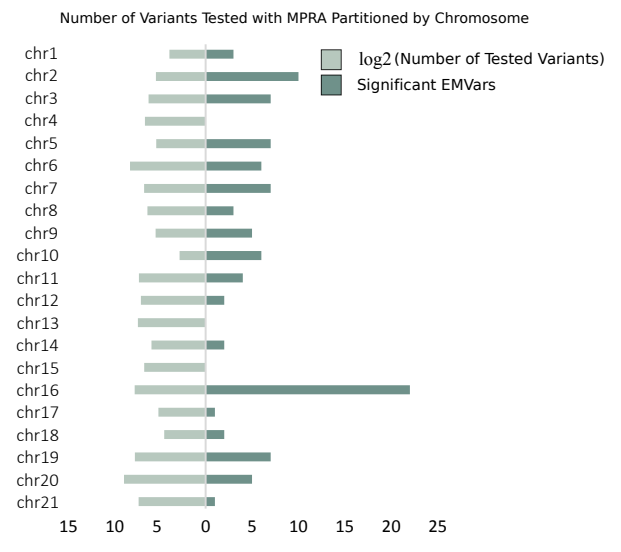
a



b



c



Supplementary Figure 6

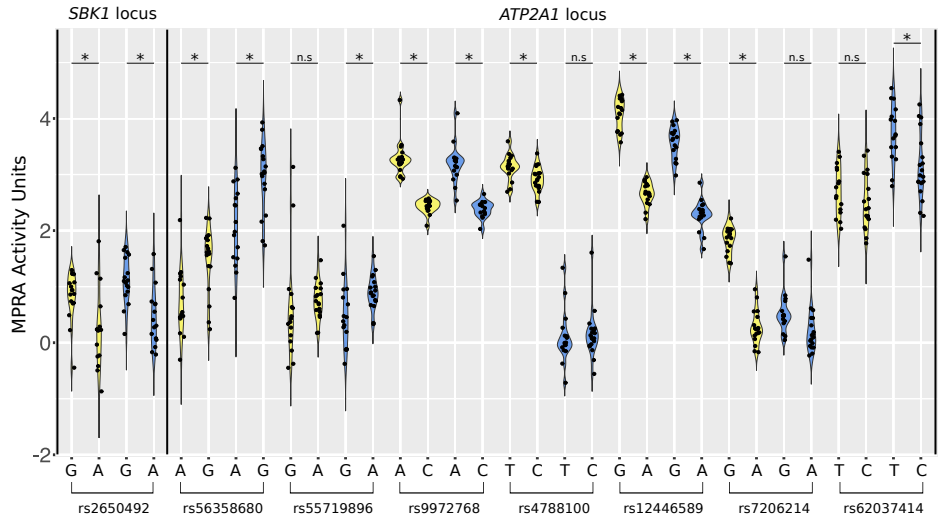
a

	GTEX eQTL	chi-C interaction	Brain EMVar	Adipose EMVar
SBKI locus	rs2650492	X	X	X
	rs28685654			X
	rs6498084		X	
ATP2A1 locus	rs56358680	X	X	X
	rs57719896	X	X	X
	rs9972768	X	X	X
	rs4788100	X	X	X
	rs12446589	X	X	X
	rs7206214	X	X	X
	rs62037414	X	X	X

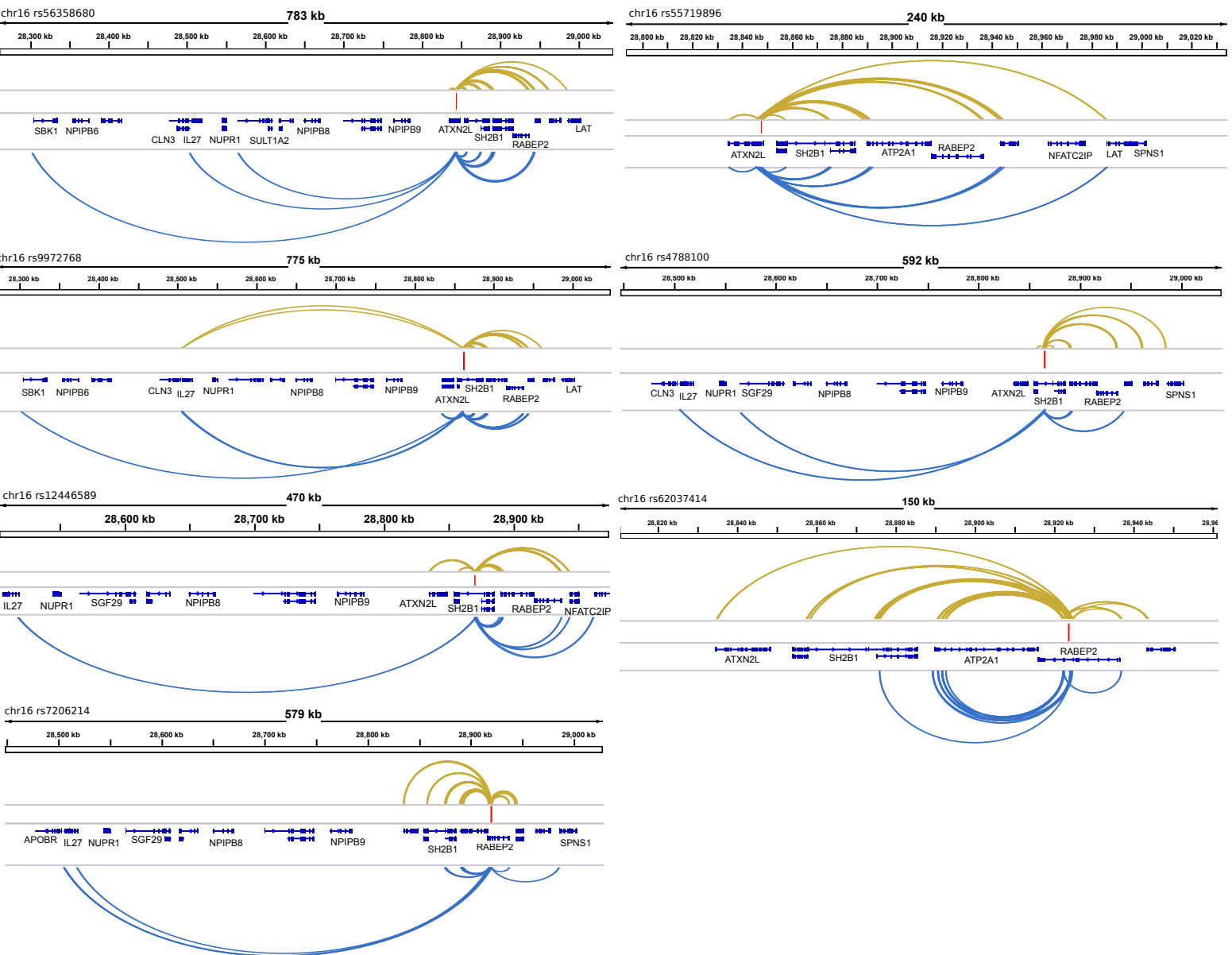
RS Number	Position (GRCh37)	Allele Frequencies	Haplotypes
rs56358680	chr16:28843118	A=0.636, G=0.364	A G G A
rs55719896	chr16:28846866	G=0.636, A=0.364	G A A G
rs9972768	chr16:28861734	A=0.636, C=0.364	A C C A
rs4788100	chr16:28864673	T=0.636, C=0.364	T C C T
rs12446589	chr16:28870962	G=0.636, A=0.364	G A A G
rs3888190	chr16:28889486	C=0.636, A=0.364	C A A C
rs7206214	chr16:28919341	G=0.667, A=0.333	G A G A
rs62037414	chr16:28923521	T=0.672, C=0.328	T C T C

Haplotype Count	124	63	8	2
Haplotype Frequency	0.6263	0.3182	0.0404	0.0101

b

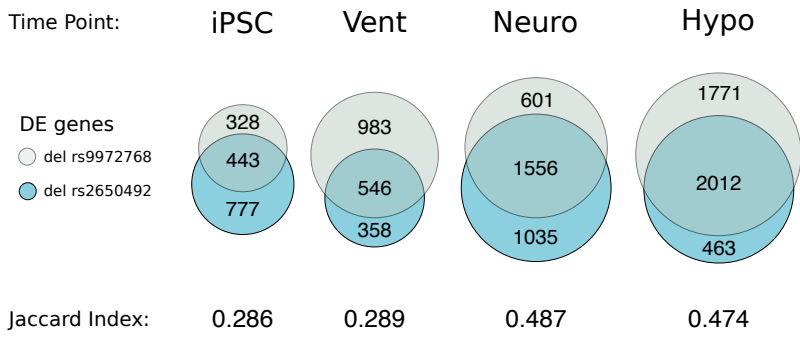


c

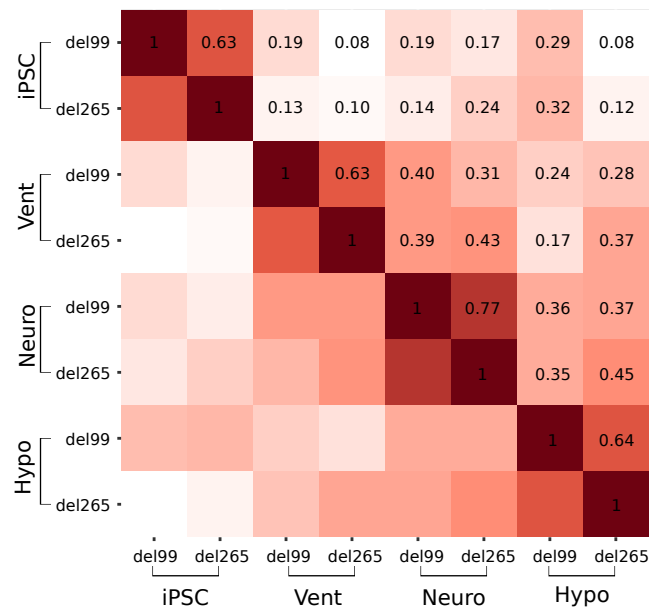


Supplementary Figure 7

a

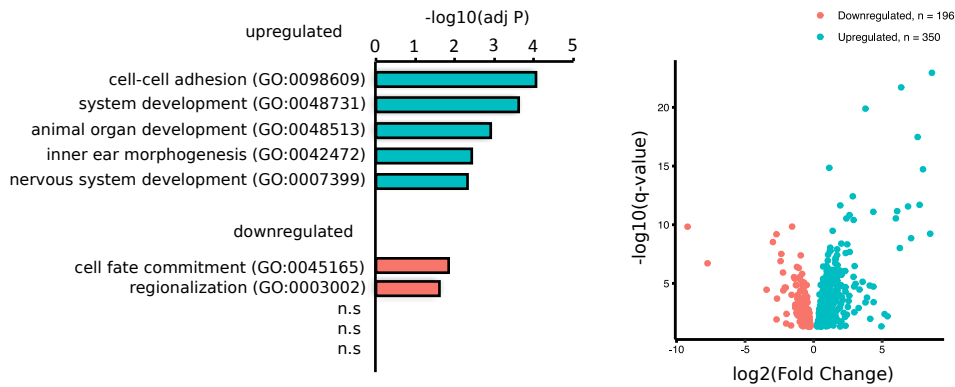


b

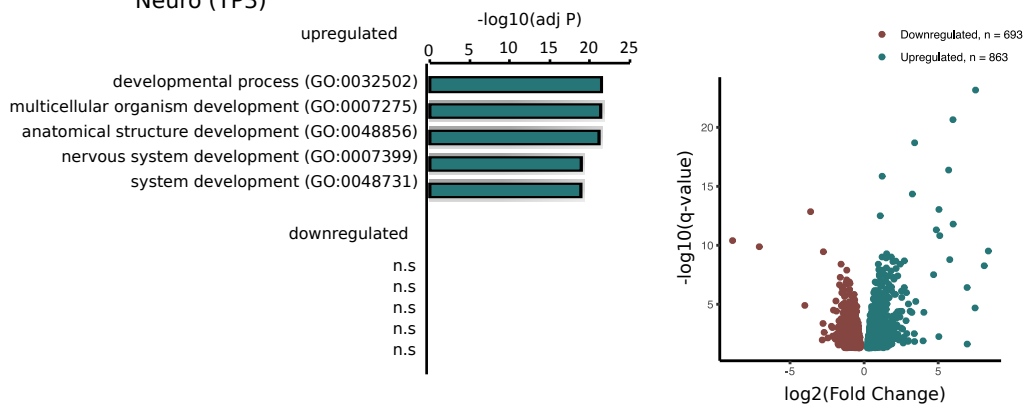


c

Vent (TP2)



Neuro (TP3)



d

